

How Do Aryl Groups Attach to a Graphene Sheet?

De-en Jiang,^{*,†,‡} Bobby G. Sumpter,^{‡,§} and Sheng Dai[†]

Chemical Sciences Division, Computer Science and Mathematics Division, and Center for Nanophase Materials Sciences, Oak Ridge National Laboratory, Oak Ridge, Tennessee 37831

Received: September 13, 2006; In Final Form: October 12, 2006

How aryl groups attach to a graphene sheet is an experimentally unanswered question. Using first principles density functional theory methods, we shed light on this problem. For the basal plane, isolated phenyl groups are predicted to be weakly bonded to the graphene sheet, even though a new single C–C bond is formed between the phenyl group and the basal plane by converting a sp^2 -carbon in the graphene sheet to sp^3 . However, the interaction can be strengthened significantly with two phenyl groups attached to the para positions of the same six-membered ring to form a pair on the basal plane. The strongest bonding is found at the graphene edges. A 1,2-addition pair is predicted to be most stable for the armchair edge, whereas the zigzag edge possesses a unique localized state near the Fermi level that shows a high affinity for the phenyl group.

1. Introduction

Carbon-based materials have found an enormously wide range of practical applications. In particular, they have played a crucial role in fuel cells, molecular electronics, separations, and catalytic systems. One important means to further expand their potential is to functionalize their surfaces. A versatile and facile method of achieving functionalization is by the reduction of diazonium salts through either electrochemical¹ or direct chemical grafting processes.² This method can covalently attach one or multiple layers of aryl groups on the carbon surface and has been applied to many allotropes of carbon.^{1–9} Recently, it has been extended to various semiconducting and metallic substrates.^{10–16} First principles density functional theory (DFT) methods have also been used to elucidate structures of chemisorbed aryl groups on transition-metal surfaces.¹⁷

During the grafting process, the aryl diazonium cation obtains one electron from either the electrode or the substrate and subsequently becomes an aryl radical by losing a dinitrogen molecule. The radical then attaches to the electrode or substrate surface.¹⁸ Because the basal plane of graphite is usually assumed to be inert due to the stability of the extended delocalized π -system, whether the aryl radical can attach to it is an intriguing yet fundamental question. Several groups reported the diazonium grafting on highly oriented pyrolytic graphite (HOPG, man-made graphite) but reached rather different conclusions. On the basis of scanning tunneling microscopy (STM) images, Pinson and co-workers³ stated that the basal plane of HOPG can be homogeneously covered with a layer of aryl groups. However, the STM images were at fairly low resolution, making their conclusion uncertain. On the basis of Raman spectroscopy studies, Liu and McCreery¹⁹ stated that the nitrophenyl group

reacts with both edge-plane and basal-plane sites, and later, Ray and McCreery²⁰ showed that the edge sites are more reactive. Also using STM, Kariuki and McDermott²¹ observed tree-like growth of aryl groups sporadically on the basal plane of HOPG after saturation of the edge sites, which could only be explained by the attack of aryl groups at the defect sites on the basal plane. In agreement with Kariuki and McDermott's results, Holm et al.²² observed the formation of islands of the grafted organic groups on the basal plane of HOPG using STM. However, they found a monolayer instead of multiple layers of grafted groups, which is likely due to their early termination of the grafting process.

Recent experiments have been focused on carbon materials such as glassy carbons (GC),^{7,22–25} carbon fiber,^{26–28} pyrolyzed photoresist films,^{29–32} carbon nanotubes,^{4,5} and porous carbons,^{8,9} which all have higher reactivity toward the diazonium grafting than HOPG. Results from time-of-flight secondary ion mass spectroscopy (ToF-SIMS) suggest covalent C–C bonding between aryl groups and the GC surface.⁷ However, similar experiments have not been performed for HOPG. From our review of the literature on HOPG (see the preceding paragraph), one can see that it is still unclear whether the aryl radical can attach to the pristine basal plane of graphite. Because graphene is the common structural basis to build up sp^2 -carbon based materials, we believe it is necessary to start with a graphene sheet in our efforts to understand the functionalization of graphite and other carbon materials by diazonium grafting. To this end, we present results obtained from a first principles DFT study of the interaction of aryl groups with a graphene sheet (our model for the basal plane of graphite). In addition, we also investigated the effect of edge sites for the aryl attachment because they are shown to be more reactive than the basal plane.

2. Theoretical Methods

The Vienna ab initio simulation package (VASP)^{33,34} was used to perform DFT calculations with planewave bases and

* To whom correspondence should be addressed. E-mail: jiangd@ornl.gov.
Phone: (865) 574-5199. Fax: (865) 576-5235.

[†] Chemical Sciences Division.

[‡] Computer Science and Mathematics Division.

[§] Center for Nanophase Materials Sciences.

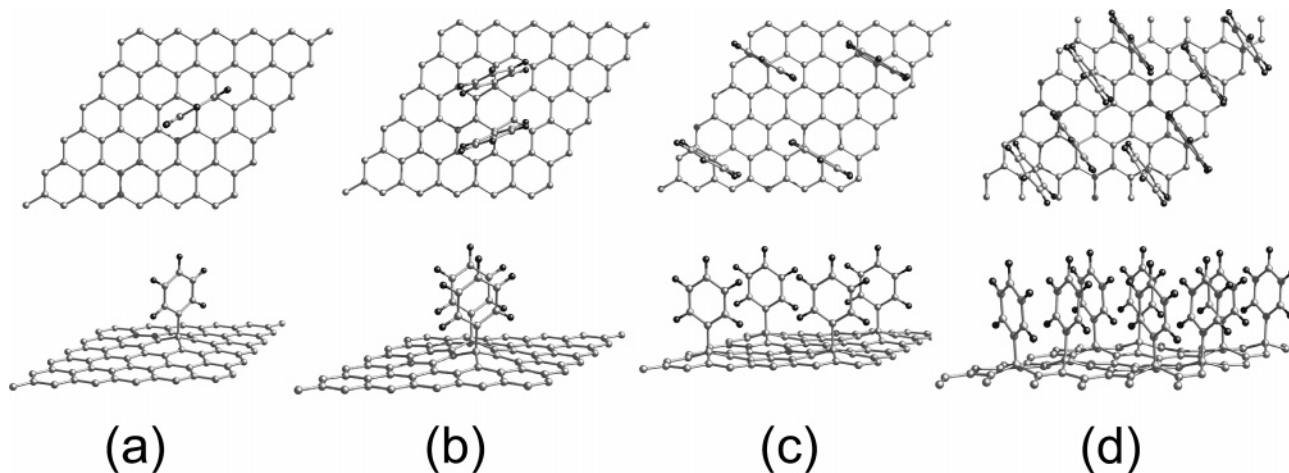


Figure 1. Optimized structures of phenyl groups on a pristine graphene sheet. From a to d, coverage increases from 0.088 to 0.70 nmol/cm² (see Table 1). In c and d, the unit cell repeats twice along the two lateral vectors. The upper panel is top view, and the bottom panel is side view. C atoms are shown in gray, and H atoms are in black. The same color scheme is used in Figure 3.

periodic boundary conditions and within the generalized-gradient approximation (GGA) for electron exchange and correlation.³⁵ The projector-augmented wave (PAW) method^{36,37} was used within the frozen core approximation to describe the electron–core interaction. A slab model was used for the graphene sheet with an optimized C–C bond length (1.426 Å) and a 16-Å vacuum layer separating the sheets. A ribbon model was used for the graphene with edge sites, with a 10-Å vacuum layer separating two neighboring edges. Depending on the system (with or without edges) and the coverage of the phenyl group, the number of atoms in the unit cell ranges from 29 to 94 (see the Supporting Information for structures presented in this work). All atoms in the unit cell were allowed to relax, and the force tolerance was set at 0.025 eV/Å. A kinetic energy cutoff of 450 eV was used, and Monkhorst-Pack k-meshes were employed to sample the Brillouin zone of all unit cells. Uncertainty in the interaction energy between the phenyl group and the graphene sheet, due to the kinetic energy cutoff and the k-point sampling, was estimated to be ~2 kJ/mol. Spin-polarized calculations were performed for the unit cells containing only one C₆H₅ group. The local magnetic moment (that is, net spin polarization on an atom) was obtained by integrating the local density of states up to the Fermi level for spin-up and spin-down states separately and then taking the difference between the two. The accuracy of our method was benchmarked against a recent study,³⁸ where pure and hybrid DFT methods and high-order correlated wavefunction methods (employing a cluster model and Gaussian-type basis sets) were used to determine the reaction energy for the attachment of CH₃ to benzene. Our result (–59 kJ/mol) compares very well with their DFT (–54 ~ –64 kJ/mol) and wavefunction (–48 ~ –59 kJ/mol) results.

3. Results and Discussion

We started with a low coverage of the phenyl group (C₆H₅) on a graphene sheet (Figure 1a) and found that the adsorption energy (E_{ad}) of attaching C₆H₅ to the graphene sheet is small (Table 1), that is, the interaction between the aryl group and the graphene sheet is weak, comparable to typical physisorption. This weak interaction indicates that an attack of the pristine graphene sheet by the C₆H₅ radical is difficult at low coverages where C₆H₅ tends to be isolated. In the optimized structure, the C–C bond that is formed has a length of 1.60 Å and the graphene carbon is displaced out of the surface by ~0.7 Å, converting into a sp³ carbon and thereby causing strain in the

TABLE 1: Energetics of the Phenyl Group (C₆H₅) on a Pristine Graphene Sheet

| structure | coverage (nmol/cm ²) | attachment (C ₆ H ₅ /cell) | E_{ad} (kJ/mol) ^a |
|-----------|----------------------------------|--|---------------------------------------|
| Figure 1a | 0.088 | 1 | –24 |
| Figure 1b | 0.175 | 2 | –123 |
| Figure 1c | 0.35 | 1 | –21 |
| Figure 1d | 0.70 | 2 | –105 |

^a $E_{\text{ad}} = E(\text{C}_6\text{H}_5/\text{graphene}) - E(\text{graphene}) - E(\text{C}_6\text{H}_5)$ for the first attachment, $E_{\text{ad}} = E(2\text{C}_6\text{H}_5/\text{graphene}) - E(\text{C}_6\text{H}_5/\text{graphene}) - E(\text{C}_6\text{H}_5)$ for the second attachment. The same definition is used in Table 2.

TABLE 2: Energetics of the Phenyl Group (C₆H₅) on a Graphene Sheet with Edge Sites

| structure | edge type | coverage (molecule/nm) | attachment (C ₆ H ₅ /cell) | E_{ad} (kJ/mol) |
|-----------|-----------|------------------------|--|--------------------------|
| Figure 3b | armchair | 0.78 | 1 | –107 |
| Figure 3c | armchair | 1.56 | 2 | –264 |
| Figure 3e | zigzag | 0.68 | 1 | –265 |
| Figure 3f | zigzag | 1.36 | 2 | –209 |

graphene sheet. The interaction energy weakly depends on the azimuthal angle of the C₆H₅ plane with respect to the graphene sheet and becomes slightly weaker when the coverage is increased (Table 1 and Figure 1c), most likely due to larger strain at the higher coverage.

The attachment of the first C₆H₅ group results in an unpaired electron on the graphene sheet. By obtaining local magnetic moments on each graphene carbon, we found that the unpaired electron is not centered on one specific graphene carbon but is distributed among many carbon atoms. Comparing different binding sites for the second attachment (Figure 2), we found that the largest energy gain is achieved by attaching the second C₆H₅ at the para position of a graphene ring (Figures 1b and d, and 2c), followed by the ortho position (Figure 2a). These two positions also have a relatively large net magnetization relative to the other binding sites, and the slightly weaker binding for the ortho position is probably due to the stronger steric repulsion between the two phenyl groups at this site. In contrast, the meta position is the least stable (Figure 2b). The energies of binding sites beyond a graphene ring of the first phenyl (Figure 2d–f) lie in between those of the para and meta positions (Figure 2b and c). For the second attachment sites on the same six-membered (C₆) ring, we see that the site at an odd-number of bonds away from the first attachment site is more stable (Figure 2a and c compared with b, and d compared with e), indicating

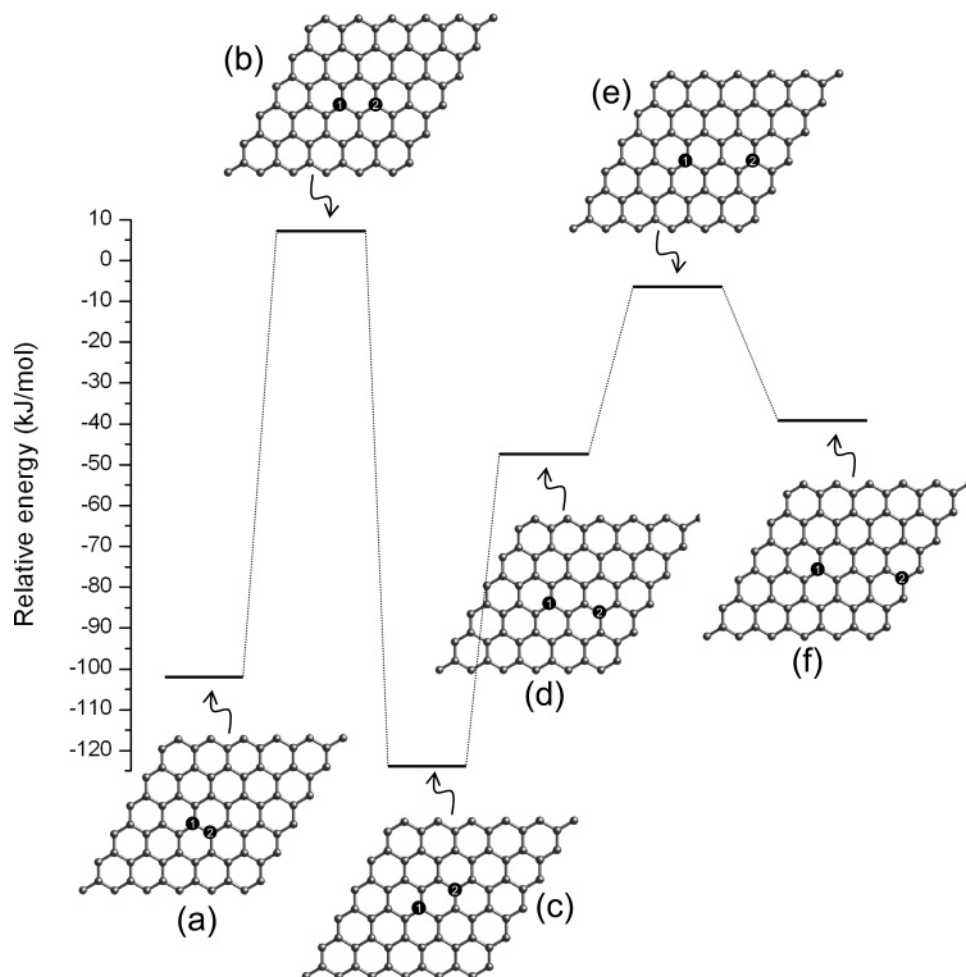


Figure 2. Structures and energetics of different sites for the second attachment of C_6H_5 on the graphene sheet. Black circles with the numbers 1 and 2 represent the site for the first and second C_6H_5 attachments, respectively. The energy is determined by $E_{\text{ad}} = E(2\text{C}_6\text{H}_5/\text{graphene}) - E(\text{C}_6\text{H}_5/\text{graphene}) - E(\text{C}_6\text{H}_5)$.

that the graphene sheet resembles a conjugated alkene chain with respect to the aryl addition.

Considering only the most stable configuration, we found that the second attachment produces an energy gain of 123 kJ/mol but decreases to 105 kJ/mol for the higher surface coverage (Table 1). Given the tendency of the PBE functional employed here to overbind,³⁹ the true interaction energy is likely to be somewhat weaker. Nevertheless, data in Table 1 indicate that C_6H_5 radicals may form a weak bonded pair on a graphene sheet and the pair's stability will decrease with surface coverage. Recently, this type of pair formation was observed using high-resolution STM for hydrogen on a graphene sheet and found to be dominant at even very low surface coverages.^{40,41} Temperature-programmed desorption (TPD) showed two peaks of recombinative H_2 (D_2) evolution: a major one at 445 (490) K and a minor one at 560 (580) K.⁴² By comparing STM images, TPD results, and DFT calculations, Hornekær et al.⁴⁰ attributed the major peak to desorption of pairs of H atoms at the para positions of the C_6 ring and the minor peak to pairs of H atoms at the ortho positions. They also showed that adsorption energies alone could not explain the double peaks and that kinetic pathways for the diffusion and the recombinative desorption had to be mapped out to understand the TPD features. Nevertheless, to obtain a reasonable idea of the temperature for desorption of a C_6H_5 pair, here we compare adsorption energies on graphene between C_6H_5 and H. Our calculations yield adsorption energies of -80 and -206 kJ/mol for the first and second (para position) H attachment on graphene, respectively.

Comparing these values to those for C_6H_5 (-24 and -123 kcal/mol), we expect that the C_6H_5 pair will desorb from the graphene sheet at temperatures significantly lower than 500 K.

Raman and STM studies^{20,21} have shown that the C_6H_5 groups first attach to the edge sites of HOPG. To compare the energetics of the basal plane with that of the edge sites, we constructed two models for the edge sites: armchair and zigzag (Figure 3a and d). The edges are passivated by atomic hydrogen.⁴³ We found that the energy gain is 107 kJ/mol for the armchair edge, whereas a much larger value of 265 kJ/mol is found for the zigzag edge. This relatively large value results directly from the presence of a localized state at the zigzag edge, which is absent in the armchair edge and the pristine graphene sheet. The local density of states for the edge carbon atoms clearly shows the origin of this difference (Figure 4). One can see a large peak near the Fermi level for the zigzag edge due to the edge state. The edge state was also predicted from a tight-binding model by Nakada et al. and confirmed recently by STM and scanning tunneling spectroscopy by Niimi et al.^{44,45} This edge state originates from the topology of the π electron system at the zigzag edge, not from dangling bonds.⁴⁴ Moreover, Nakada et al. and Niimi et al. showed that the localized edge state also appears at the zigzag segment of an edge with mixed zigzag and armchair configurations. A similar localized state also appears on the zigzag step edge of multilayer ribbons.⁴⁶ These results indicate that the localized edge state probably exists in many sp^2 -carbon based materials, such as HOPG, porous carbon, and glassy carbon.

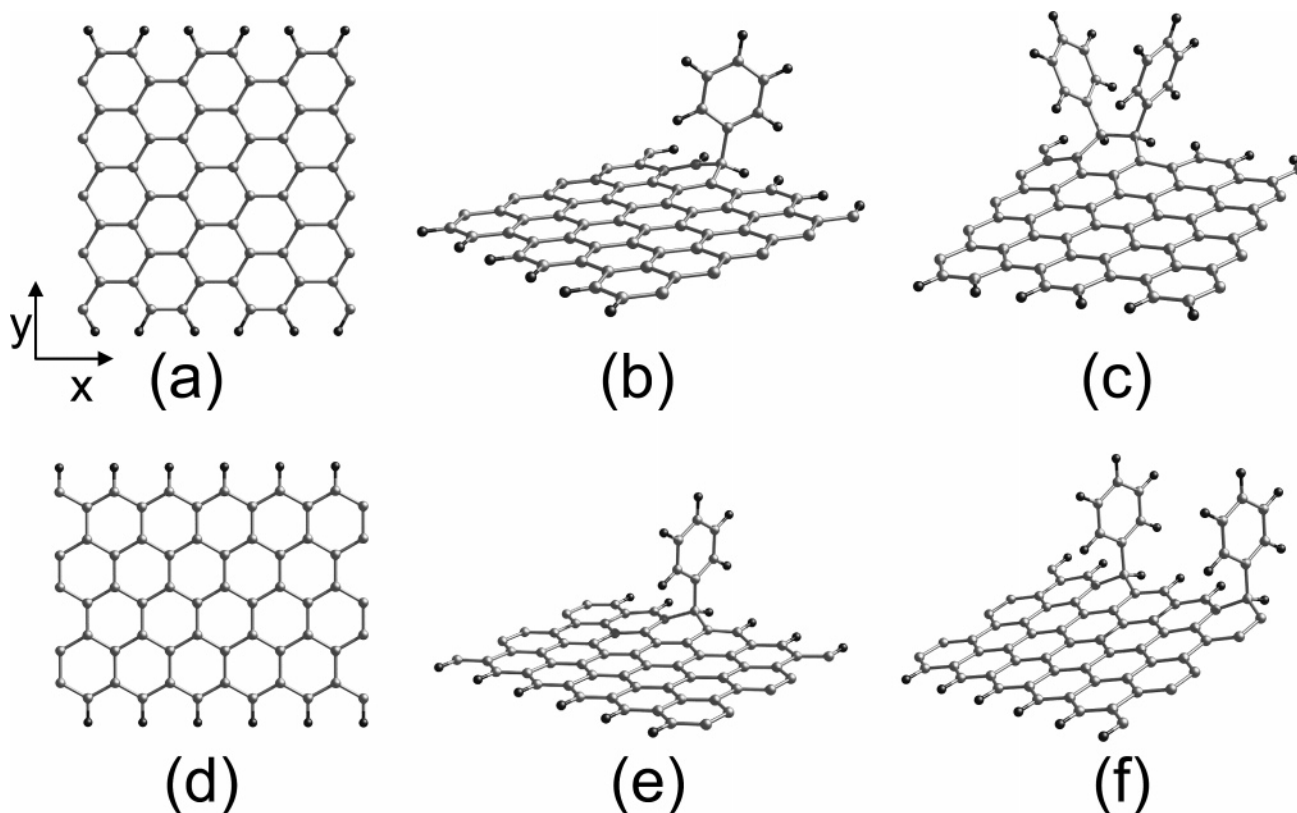


Figure 3. Models for armchair (a) and zigzag (d) edges sites of a graphene sheet and optimized structures of phenyl groups attached to the edge sites. With (a) as an example, the edge is terminated with hydrogen atoms (shown in black) and repeated infinitely along the x axis, whereas the ribbon has a chosen width along the y axis.

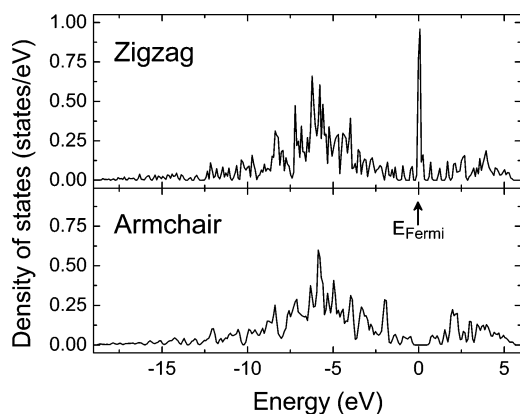


Figure 4. Local density of states of carbon atoms on the edge (that is, carbon atoms connected to hydrogen; see Figure 3a and d).

Attaching the second C_6H_5 group on the edge is also different from that on the basal plane. We found that instead of the 1,4-addition position, the second C_6H_5 radical prefers a 1,2-addition position on the armchair edge (Figure 3c) and yields an adsorption energy of -264 kJ/mol. On the zigzag edge, the second C_6H_5 chooses to be far away from the first C_6H_5 and has an adsorption energy of -209 kJ/mol. The energetic difference between zigzag and armchair edges decreases when the second C_6H_5 is attached. These large adsorption energies at the edge sites provide a rational for the high reactivity of the graphite edge toward C_6H_5 .

The higher reactivity of edge sites commonly observed in the diazonium-grafting experiments on HOPG^{3,19–21} is clearly demonstrated by our calculations. The remaining question is whether the pristine plane of the graphene sheet can be grafted by the diazonium process. Examining the experiments on the diazonium-grafting of HOPG, we feel that the STM results of

Kariuki and McDermott's²¹ offer a more direct observation of the grafting process. They observed sporadic tree-like growth of aryl films on the basal plane and concluded that grafting is most likely initiated at defect sites on the basal plane. Our calculations show that the bonding between aryl groups and a pristine graphene sheet is indeed weak, especially when the aryl groups are isolated, and therefore, support their conclusion. However, because the grafting experiment was done by an electrochemical method in a solution, direct connection between theory and experiment can be established only when the detailed mechanism of diazonium-grafting is elucidated. The modestly stable pair that we predicted on the basal plane can in principle be observed by high-resolution STM. Whether this type of pair formation can be obtained by the diazonium-grafting process is currently unclear. However, recent STM observation of islands (monolayer thick and ~ 2 nm wide) of grafted molecules on the basal plane of HOPG is an encouraging sign.²² Further controlled grafting and better resolved structures may verify our prediction.

4. Summary and Conclusions

We have studied the interaction between a phenyl group (C_6H_5) and a graphene sheet using first principles gradient-corrected density functional theory. Our results show that isolated C_6H_5 groups are weakly bonded to the basal plane, comparable to physisorption, whereas a pair of C_6H_5 molecules, located at the para positions of the same graphene ring, is significantly more stable. We also demonstrated the high reactivity of edge sites for aryl attachments: A 1,2-addition pair is predicted to be most stable for the armchair edge, whereas the zigzag edge, which possesses a unique localized state near the Fermi level, shows a higher affinity for an isolated phenyl group. Our calculations provide support for the experimental

observation that edge sites of graphite are more reactive than the basal plane during the aryl diazonium-grafting process.

Acknowledgment. This work was supported by Office of Basic Energy Sciences, U.S. Department of Energy under Contract No. DE-AC05-00OR22725 with UT-Battelle, LLC, and used resources of the National Center for Computational Sciences at Oak Ridge National Laboratory. B.G.S. acknowledges research conducted at the Center for Nanophase Materials Sciences, supported by the division of Scientific User Facilities, U.S. Department of Energy.

Supporting Information Available: Coordinates for all of the stable structures of phenyl on graphene sheets. This material is available free of charge via the Internet at <http://pubs.acs.org>.

References and Notes

- (1) Delamar, M.; Hitmi, R.; Pinson, J.; Saveant, J. M. *J. Am. Chem. Soc.* **1992**, *114*, 5883–5884.
- (2) Belmont, J. A. U.S. Patent 5,554,739, 1996.
- (3) Allongue, P.; Delamar, M.; Desbat, B.; Fagebaume, O.; Hitmi, R.; Pinson, J.; Saveant, J. M. *J. Am. Chem. Soc.* **1997**, *119*, 201–207.
- (4) Bahr, J. L.; Yang, J. P.; Kosynkin, D. V.; Bronikowski, M. J.; Smalley, R. E.; Tour, J. M. *J. Am. Chem. Soc.* **2001**, *123*, 6536–6542.
- (5) Strano, M. S.; Dyke, C. A.; Usrey, M. L.; Barone, P. W.; Allen, M. J.; Shan, H. W.; Kittrell, C.; Hauge, R. H.; Tour, J. M.; Smalley, R. E. *Science* **2003**, *301*, 1519–1522.
- (6) Dyke, C. A.; Tour, J. M. *J. Am. Chem. Soc.* **2003**, *125*, 1156–1157.
- (7) Combella, C.; Kanoufi, F.; Pinson, J.; Podvorica, F. I. *Langmuir* **2005**, *21*, 280–286.
- (8) Li, Z. J.; Yan, W. F.; Dai, S. *Langmuir* **2005**, *21*, 11999–12006.
- (9) Li, Z. J.; Dai, S. *Chem. Mater.* **2005**, *17*, 1717–1721.
- (10) Adenier, A.; Bernard, M. C.; Chehimi, M. M.; Cabet-Deliry, E.; Desbat, B.; Fagebaume, O.; Pinson, J.; Podvorica, F. *J. Am. Chem. Soc.* **2001**, *123*, 4541–4549.
- (11) Bernard, M. C.; Chausse, A.; Cabet-Deliry, E.; Chehimi, M. M.; Pinson, J.; Podvorica, F.; Vautrin-Ul, C. *Chem. Mater.* **2003**, *15*, 3450–3462.
- (12) Stewart, M. P.; Maya, F.; Kosynkin, D. V.; Dirk, S. M.; Stapleton, J. J.; McGuinness, C. L.; Allara, D. L.; Tour, J. M. *J. Am. Chem. Soc.* **2004**, *126*, 370–378.
- (13) Chen, B.; Flatt, A. K.; Jian, H. H.; Hudson, J. L.; Tour, J. M. *Chem. Mater.* **2005**, *17*, 4832–4836.
- (14) Mirkhalaf, F.; Paprotny, J.; Schiffrin, D. J. *J. Am. Chem. Soc.* **2006**, *128*, 7400–7401.
- (15) Maldonado, S.; Smith, T. J.; Williams, R. D.; Morin, S.; Barton, E.; Stevenson, K. J. *Langmuir* **2006**, *22*, 2884–2891.
- (16) Adenier, A.; Combella, C.; Kanoufi, F.; Pinson, J.; Podvorica, F. *I. Chem. Mater.* **2006**, *18*, 2021–2029.
- (17) Jiang, D. E.; Sumpter, B. G.; Dai, S. *J. Am. Chem. Soc.* **2006**, *128*, 6030–6031.
- (18) Pinson, J.; Podvorica, F. *Chem. Soc. Rev.* **2005**, *34*, 429–439.
- (19) Liu, Y. C.; McCreery, R. L. *J. Am. Chem. Soc.* **1995**, *117*, 11254–11259.
- (20) Ray, K.; McCreery, R. L. *Anal. Chem.* **1997**, *69*, 4680–4687.
- (21) Kariuki, J. K.; McDermott, M. T. *Langmuir* **1999**, *15*, 6534–6540.
- (22) Holm, A. H.; Moller, R.; Vase, K. H.; Dong, M. D.; Norrman, K.; Besenbacher, F.; Pedersen, S. U.; Daasbjerg, K. *New J. Chem.* **2005**, *29*, 659–666.
- (23) Downard, A. J. *Langmuir* **2000**, *16*, 9680–9682.
- (24) Kariuki, J. K.; McDermott, M. T. *Langmuir* **2001**, *17*, 5947–5951.
- (25) D'Amours, M.; Belanger, D. *J. Phys. Chem. B* **2003**, *107*, 4811–4817.
- (26) Coulon, E.; Pinson, J.; Bourzat, J. D.; Commercon, A.; Pulicani, J. P. *Langmuir* **2001**, *17*, 7102–7106.
- (27) Coulon, E.; Pinson, J.; Bourzat, J. D.; Commercon, A.; Pulicani, J. P. *J. Org. Chem.* **2002**, *67*, 8513–8518.
- (28) Hermans, A.; Seipel, A. T.; Miller, C. E.; Wightman, R. M. *Langmuir* **2006**, *22*, 1964–1969.
- (29) Anariba, F.; DuVall, S. H.; McCreery, R. L. *Anal. Chem.* **2003**, *75*, 3837–3844.
- (30) Brooksby, P. A.; Downard, A. J. *Langmuir* **2004**, *20*, 5038–5045.
- (31) Brooksby, P. A.; Downard, A. J. *J. Phys. Chem. B* **2005**, *109*, 8791–8798.
- (32) Anariba, F.; Viswanathan, U.; Bocian, D. F.; McCreery, R. L. *Anal. Chem.* **2006**, *78*, 3104–3112.
- (33) Kresse, G.; Furthmüller, J. *Phys. Rev. B* **1996**, *54*, 11169–11186.
- (34) Kresse, G.; Furthmüller, J. *Comp. Mater. Sci.* **1996**, *6*, 15–50.
- (35) Perdew, J. P.; Burke, K.; Ernzerhof, M. *Phys. Rev. Lett.* **1996**, *77*, 3865–3868.
- (36) Blöchl, P. E. *Phys. Rev. B* **1994**, *50*, 17953–17979.
- (37) Kresse, G.; Joubert, D. *Phys. Rev. B* **1999**, *59*, 1758–1775.
- (38) Unterreiner, B. V.; Carissan, Y.; Kloppe, W. *ChemPhysChem* **2006**, *7*, 1311–1321.
- (39) Hammer, B.; Hansen, L. B.; Nørskov, J. K. *Phys. Rev. B* **1999**, *59*, 7413–7421.
- (40) Hornekaer, L.; Sljivancanin, Z.; Xu, W.; Otero, R.; Rauls, E.; Stensgaard, I.; Laegsgaard, E.; Hammer, B.; Besenbacher, F. *Phys. Rev. Lett.* **2006**, *96*, 156104.
- (41) Andree, A.; Le Lay, M.; Zecho, T.; Kupper, J. *Chem. Phys. Lett.* **2006**, *425*, 99–104.
- (42) Zecho, T.; Guttler, A.; Sha, X. W.; Jackson, B.; Kuppers, J. *J. Chem. Phys.* **2002**, *117*, 8486–8492.
- (43) The hydrogen atoms are used only to passivate the dangling bonds on the edge carbon atoms. The mechanism that aryl groups abstract H from edge C–H bonds is not considered here.
- (44) Nakada, K.; Fujita, M.; Dresselhaus, G.; Dresselhaus, M. S. *Phys. Rev. B* **1996**, *54*, 17954–17961.
- (45) Kobayashi, Y.; Fukui, K.; Enoki, T.; Kusakabe, K. *Phys. Rev. B* **2006**, *73*, 125415.
- (46) Miyamoto, Y.; Nakada, K.; Fujita, M. *Phys. Rev. B* **1999**, *59*, 9